



Numerical Analysis for Energy Transfer Analysis of Micropolar Nanofluid by Keller Box Scheme

Khuram Rafique^{1*}, Nida Ibrar², Ayesha Munir¹, Adeel Khalid³, Ayesha Ijaz³ and Asma Asghar³

¹Department of Mathematics, University of Sialkot, Sialkot, Pakistan

²Department of Mathematics, University of Sargodha, Pakistan

³Department of Zoology, University of Sialkot, Pakistan

*Corresponding Author: Khurame Rafique, Department of Mathematics, University of Sialkot, Sialkot, Pakistan.

Received: January 20, 2023

Published: February 15, 2023

© All rights are reserved by Khuram Rafique., et al.

Abstract

This Research conducted for the micro-rotational flow of nanoliquid over an extendable surface. In current era dispersion of nano particles in the regular liquids have become a significant importance in nanotechnology. Nanoparticles dispersion improve the thermal conductivity of the regular liquid which is very helpful for energy production and transmission. The transportation of energy has been taken as a key factor of investigation in this research. In this study thermal radiations and Dufour impacts have been utilized. Moreover, the Dufour effects are also considered. The well-known computational scheme of Keller Box (KBS) has been used in this work. More exactly, in this work, the Buongiorno model is considered for the numerical investigation. The flow equations are transformed into the nonlinear differential equation by employing an appropriate similarity transformations. The physical quantities with several effects of material constraints are portrayed in the form of graphs and tables. It is found that inclination impact causes reduction in velocity profile.

Keywords: MHD; KBS; Thermal Radiations; Dufour Effects; Micropolar Nanofluid; Inclined Surface

Introduction

The present world, in light of regularly growing utilization of thermal energy management, becomes serious and challenging. The potential structures of nanotechnology and nanoscience to improve the pace of heat extraction from the inevitable sources have pulled in various analysts. Besides, nanofluids have presented vast extent of advantageous applications, for instance, brain tumor injection, cancer identification, sun oriented vitality, high control lasers, and penetrating.

Moreover, in existing work, there are a few procedures that intention to improve the heat exchange factor in the flow to upgrade the capability of concentrating collector. Nanoparticles have more prominent thermal conductivity as equated with base liquids, the idea of submerging stable nanoparticles in the base liquids was experienced. Nanoliquids improve the productivity of the solar system because of their predominant thermal attributes. The term nano was first presented by Choi [1]. Pak and Cho [2] scrutinized

the energy transportation of base fluid by immersing the submicron metallic oxide and determined that the energy exchange improvement depends on the thermal conductivity and size of the particles. In previous centuries, several academic studies are stated on the flow of nanofluids. The core subjects of these studies are, the employment of effective thermal conductivity and the effective viscosity in the energy and momentum equations, including the slip mechanisms between the nanoparticles and base liquid molecules (see Buongiorno [3]). The researchers have investigated the flow of nanofluids by using both methodologies. For more literature on nanofluid flow on a slanted surface, see [4-9].

The effects of thermal radiations on the flow and heat transportation have considerably fascinated the attention of experts and investigators. It is due to their remarkable applications in solar technology, in production and quantum mechanics, and particularly in high heat processes. These influences may also include an essential portion of the dynamics controlling the energy exchange in the

industry where the excellence of the last piece depends upon the temperature adjusting mechanisms to some extent. Sandeep and Kumar [10] inspected the influence of the radiation on the nanofluid flow towards an inclined sheet. Later on, Govindrajan and Rani [11] examined inclination influence on the nanofluid flow with radiative impacts. Also, Khan., *et al.* [12] discussed Carreau nanofluid flow on an enlarging cylinder with an inclination effect. Recently, the investigation of radiation effects on the Casson nanofluid flow over an inclined disk investigated by Saeed., *et al.* [13]. Besides, different researchers investigated the radiation's effects on the nanofluid flow with different geometries, see [14-19].

The flow performance of non-Newtonian liquid is an investigation of the profound fascination of researchers and practical importance. There are a couple of ordinary and mechanical usages of such liquids, liquid polymers, infiltrating mud, oils, specific coats, molten suspensions, nourishment items and curative and various others. In literature, there are several statistical models with different constitutive settings containing a unique set of rigorous factors. The micropolar liquid model is appropriate for exocitic oils, blood of animal, liquid minerals with firm atoms, specific biological solutions, and colloidal solutions. The micromotion of liquid components, spin inertia, and the impacts of the couple stresses are very essential in micropolar liquids. Eringen [20] presented the idea of micropolar liquids based on constitution equations. For in depth study on the micropolar nanofluid flow by considering several geometries see [21-29].

The assessed literature reveals that no investigation till now has been done in the direction concerning micropolar nanofluid flow on inclined surface with radiations and Soret, Dufour effects. Therefore, here we have offered the numerical simulation to tackle the features of micropolar type nanofluid flow towards an inclined sheet by employing KBS. The graphical diagrams are provided to demonstrate the effect logs of our concern parameters on temperature, velocity, and concentration contours. The current outcomes are novel.

Mathematical formulation

This study is focused with the radiations and Soret effects on micropolar nanofluid flow on a slanted surface. Flow made due to linear stretching with a stretching rate ' b '. The surface is slanted with an inclination Ω . Brownian motion and thermophoretic influences are incorporated. The magnetic field is considered perpendicular the slanted surface.

The governing equations for the flow under consideration are:

$$\frac{\partial u}{\partial x} + \frac{\partial v}{\partial y} = 0, \text{ ----- (1)}$$

$$u \frac{\partial u}{\partial x} + v \frac{\partial v}{\partial y} = \left(\frac{\mu + k_1^*}{\rho} \right) \frac{\partial^2 u}{\partial y^2} + \left(\frac{k_1^*}{\rho} \right) \frac{\partial N^*}{\partial y} + g[\beta_t(T - T_\infty) + \beta_c(C - C_\infty)] \cos \Omega - \frac{\sigma B_0^2}{\rho} u, \text{ ----- (2)}$$

$$u \frac{\partial N^*}{\partial x} + v \frac{\partial N^*}{\partial y} = \left(\frac{\gamma^*}{j^* \rho} \right) \frac{\partial^2 N^*}{\partial y^2} - \left(\frac{k_1^*}{j^* \rho} \right) \left(2N^* + \frac{\partial u}{\partial y} \right), \text{ ----- (3)}$$

$$u \frac{\partial T}{\partial x} + v \frac{\partial T}{\partial y} = \alpha \frac{\partial^2 T}{\partial y^2} - \frac{1}{(\rho c)_f} \frac{\partial q_r}{\partial y} + \tau \left[D_B \frac{\partial C}{\partial y} \frac{\partial T}{\partial y} + \frac{D_T}{T_\infty} \left(\frac{\partial T}{\partial y} \right)^2 \right] + \frac{D_T K_T}{C_s C_p} \frac{\partial^2 C}{\partial y^2}, \text{ ----- (4)}$$

$$u \frac{\partial C}{\partial x} + v \frac{\partial C}{\partial y} = D_B \frac{\partial^2 C}{\partial y^2} + \frac{D_T K_T}{T_\infty} \frac{\partial^2 T}{\partial y^2}. \text{ ----- (5)}$$

Where, the Rosseland approximation characterized as

$$q_r = -\frac{4\sigma^*}{3k^*} \frac{\partial T^4}{\partial y}. \text{ ----- (6)}$$

Where σ^* stands for the Stefan-Boltzmann coefficient and k^* denotes mean absorption coefficient. By applying Taylers series the expansion of T^4 in terms of T_∞ written as:

$$T^4 \cong 4T_\infty^3 T - 3T_\infty^4, \text{ ----- (7)}$$

By using equations (5) and (6) the equation (3) converted into:

$$u \frac{\partial T}{\partial x} + v \frac{\partial T}{\partial y} = \left(\alpha + \frac{16\sigma^* T_\infty^3}{3k^* (\rho c)_f} \right) \frac{\partial^2 T}{\partial y^2} + \tau \left[D_B \frac{\partial C}{\partial y} \frac{\partial T}{\partial y} + \frac{D_T}{T_\infty} \left(\frac{\partial T}{\partial y} \right)^2 \right], \text{ ----- (8)}$$

The boundary settings are

$$\begin{aligned} v = 0, u = b, N^* = -m \frac{\partial u}{\partial y}, T = T_w, C = C_w, \text{ at } y = 0, \\ v \rightarrow 0, u \rightarrow u_\infty = 0, N^* \rightarrow 0, T \rightarrow T_\infty, C \rightarrow C_\infty, \text{ as } y \rightarrow \infty. \end{aligned} \text{ ----- (9)}$$

The stream function $\psi = \psi(x, y)$ is defined by

$$u = \frac{\partial \psi}{\partial y}, \quad v = -\frac{\partial \psi}{\partial x}. \quad (10)$$

The similarity transformations are expressed by

$$u = bxf(\eta), \quad \eta = y\sqrt{\frac{b}{\nu}}, \quad v = -\sqrt{b\nu}f'(\eta)$$

$$N^* = b\left(\sqrt{\frac{b}{\nu}}\right)h(\eta), \quad \theta(\eta) = \frac{T - T_\infty}{T_w - T_\infty}, \quad \phi(\eta) = \frac{C - C_\infty}{C_w - C_\infty}.$$

----- (11)

By employing equation (11), equations (2), (3), (8) and (5) becomes

$$(1 + K)f'''' + f'' - f'^2 + K' + (G_x\theta + G_c\phi)\cos\Omega - M(f') = 0,$$

----- (12)

$$\left(1 + \frac{K}{2}\right)h'' + fh' - f'h - K(2h + f'') = 0, \quad (13)$$

$$P_N\theta'' + f\theta' + N\phi'\theta' + N\theta'^2 + D_f\phi'' = 0, \quad (14)$$

$$\phi'' + Le f\phi' + SrLe\theta'' = 0. \quad (15)$$

Where,

$$\text{Magnetic parameter : } M = \frac{\sigma B_0^2}{a\rho},$$

$$\text{Brownian motion factor : } N = \frac{\tau D_B (C_w - C_\infty)}{\nu},$$

$$\text{Thermophoresis factor : } N = \frac{\tau D_T (T_w - T_\infty)}{\nu T_\infty},$$

$$\text{Local Grashof number : } G_x = \frac{g\beta_c (T_w - T_\infty)x^{-1}}{a^2},$$

$$\text{Local modified Grashof number : } G_x = \frac{g\beta_c (C_w - C_\infty)x^{-1}}{a^2},$$

$$\text{Modified Prandtl number : } P_N = \frac{1}{P} \left(1 + \frac{4}{3}N\right),$$

$$\text{Dufour effect : } D_f = \frac{D_T K_T (C_w - C_\infty)}{\nu C_s C_p (T_w - T_\infty)},$$

$$\text{Soret effect : } S = \frac{D_T K_T (T_w - T_\infty)}{\nu T_\infty (C_w - C_\infty)}.$$

Here, to find similarity solution G_x and G_c should be without X . Hence, suppose that [30,31].

$$\beta_l = n^{-1}, \beta_c = n_1 x^1. \quad (16)$$

Where n_1 and n denotes constants. Replacing equation (17) in to the parameters and , results become

$$G_x = \frac{g_1 (C_w - C_\infty)}{a^2}, \quad G_c = \frac{g (T_w - T_\infty)}{a^2}. \quad (17)$$

The conditions at the boundary are converted into

$$f(\eta) = 0, \quad f'(\eta) = 1, \quad h(\eta) = 0, \quad \theta(\eta) = 1, \quad \phi(\eta) = 1, \quad \text{at } \eta = 0,$$

$$f'(\eta) \rightarrow 0, \quad h(\eta) \rightarrow 0, \quad \theta(\eta) \rightarrow 0, \quad \phi(\eta) \rightarrow 0, \quad \text{at } \eta \rightarrow \infty.$$

----- (18)

The associated expressions of $C_{fx}(0) = (1 + K)f''(0)$, $-\theta'(0)$, and $-\phi'(0)$ (skin friction, Nusselt number, and Sherwood number) becomes

$$-\theta'(0) = \frac{Nu_x}{\left(1 + \frac{4}{3}N\right)\sqrt{Re_x}}, \quad -\phi'(0) = \frac{Sh_x}{\sqrt{Re_x}}, \quad C_{fx} = C_f \sqrt{Re_x},$$

----- (19)

Results and Discussion

This portion of article exhibited different graphs and tables for physical parameters containing magnetic factor M , local Grashof number G_r , local modified Grashof number G_c , inclination i.e. Ω , P_r (Prandtl number), radiation effect N , Soret factor S_r , Dufour parameter D_f , Lewis number L_e , Brownian motion i.e. Nb , thermophoresis i.e. Nt , and material factor K . To match current outcomes with already published results of Khan and Pop [32] prepared Table 1, in the absence of $D_f, Gr, Sr, N, M, G_c, K$ and $Pr = Le = 10$ and with . Table 2 shows the variations in $-\theta'(0)$, $\phi'(0)$ and in $C_{fx}(0)$.

In Table 3.2 bold parameters presents the change in that particular parameter value how energy and mass flux along with skin friction vary.

Figure 1 portrays the velocity field behavior against magnetic field effect. It demonstrates that $f'(\eta)$ reduces on improving the magnetic field strength. Physically, velocity profile declines on the growth of the magnetic factor because resistive force (Lorentz force). The velocity profile increases with changed numerics of local Grashof number see (Figure 2). Physically, the viscous force declines by growing magnitude of the buoyancy forces. Figure 3 $f'(\eta)$ follow the same shape on the increment of local modified Grashof number as like local Grashof number effect in figure 2. Figure 4 reveals the inclination impact on the velocity profile. It demonstrated that $f'(\eta)$ enhances on growing angle. The buoyancy force diminishes at $\Omega = 90^\circ$ which causes a reduction in the velocity profile.

Figure 5 shows the influence of the material parameter on velocity profile. It is found that velocity field for the altered values of K increases. Physically, the increment in the material factor drops the viscosity and raises the velocity. The magnetic effect impression on $h'(\eta)$ offered in Figure 6. The angular velocity decreases against changed numerics of magnetic factor.

On the other hand, against the higher magnitude of the factor, K the angular velocity upturn (see Figure 7). This demonstration corresponds with the outcomes of Rafique., *et al.* [21]. Figure 8 express the impact of radiation on the temperature distribution. Physically the conductive heat transfer is larger than the radiative heat exchange, which reasons behind the lessening of boundary layer thickness and buoyancy force. The liquid becomes warmer against the increment in the radiations due to which the energy flux enhances. The energy and mass flux rates along skin friction are portrayed in Figures 9-14 for distinct magnitudes of N , Ω and N . Figures 9 and 10 exhibit the energy and mass fluxes diminish with growing of Brownian motion and inclination effect.

Moreover, the skin friction increases against cumulative magnitudes of Brownian motion and inclination effect portrayed in Figure 11. Further, heat and mass fluxes are descents compared to the cumulative magnitudes of thermophoretic and inclination parameters (see Figures 12-13). While, wall shear stress improved on growth of inclination and thermophoretic influences (see Figure 14).

Table 1: Contrast of $-\theta'(0)$ and $-\phi'(0)$ against $M, N, Sr, Df, K, Gr, Gc = 0$ with $Le, Pr = 10$ and $\Omega = 90^\circ$.

Nb	Nt	Present Results		Khan and Pop [32]	
		$-\theta'(0)$	$-\phi'(0)$	$-\theta'(0)$	$-\phi'(0)$
0.1	0.1	0.9524	2.1294	0.9524	2.1294
0.2	0.2	0.3654	2.5152	0.3654	2.5152
0.3	0.3	0.1355	2.6088	0.1355	2.6088
0.4	0.4	0.0495	2.6038	0.0495	2.6038
0.5	0.5	0.0179	2.5731	0.0179	2.5731

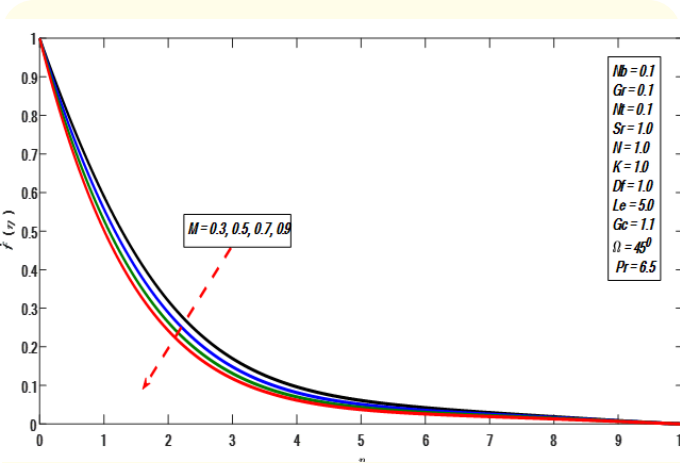


Figure 1: $f'(\eta)$ versus M .

<i>Nb</i>	<i>Nt</i>	<i>Pr</i>	<i>Le</i>	<i>M</i>	<i>K</i>	<i>Gr</i>	<i>Gc</i>	<i>Sr</i>	<i>Df</i>	<i>N</i>	Ω	$-\theta'(0)$	$-\phi'(0)$	$C_{fx}(0)$
0.1	0.1	6.5	5.0	0.2	1.0	0.1	1.1	1.0	1.0	1.0	45°	0.5641	0.5100	0.9362
0.3	0.1	6.5	5.0	0.2	1.0	0.1	1.1	1.0	1.0	1.0	45°	0.6167	0.4552	0.8998
0.1	0.3	6.5	5.0	0.2	1.0	0.1	1.1	1.0	1.0	1.0	45°	0.4842	0.4702	0.9484
0.1	0.1	10.0	5.0	0.2	1.0	0.1	1.1	1.0	1.0	1.0	45°	0.5588	0.5380	0.9640
0.1	0.1	6.5	10.0	0.2	1.0	0.1	1.1	1.0	1.0	1.0	45°	0.6162	0.5058	0.9171
0.1	0.1	6.5	5.0	0.5	1.0	0.1	1.1	1.0	1.0	1.0	45°	0.5469	0.4954	1.1289
0.1	0.1	6.5	5.0	0.2	3.0	0.1	1.1	1.0	1.0	1.0	45°	0.5876	0.5299	1.3739
0.1	0.1	6.5	5.0	0.2	1.0	0.5	1.1	1.0	1.0	1.0	45°	0.5752	0.5195	0.7731
0.1	0.1	6.5	5.0	0.2	1.0	0.1	2.0	1.0	1.0	1.0	45°	0.5916	0.5336	0.5568
0.1	0.1	6.5	5.0	0.2	1.0	0.1	1.1	2.0	1.0	1.0	45°	0.3750	0.4878	0.9930
0.1	0.1	6.5	5.0	0.2	1.0	0.1	1.1	1.0	2.0	1.0	45°	0.5829	0.3954	0.8267
0.1	0.1	6.5	5.0	0.2	1.0	0.1	1.1	1.0	1.0	2.0	45°	0.5687	0.4646	0.8925
0.1	0.1	6.5	5.0	0.2	1.0	0.1	1.1	1.0	1.0	1.0	90°	0.5009	0.4129	1.4990

Table 2: Values of $-\theta'(0)$, $-\phi'(0)$ and $C_{fx}(0)$.

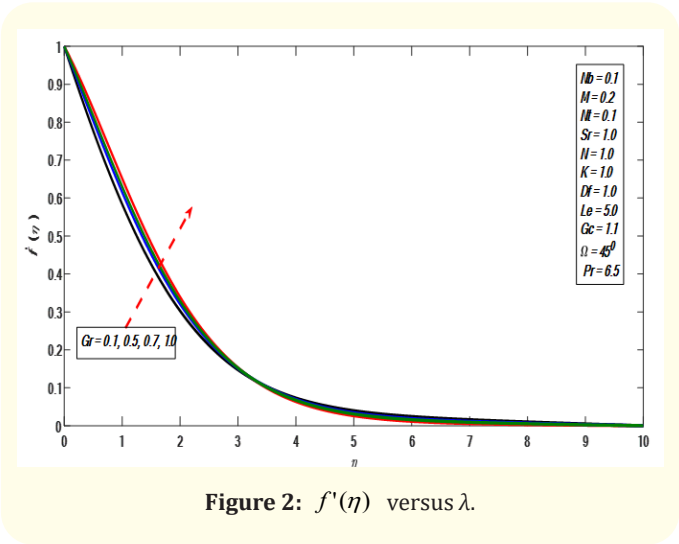


Figure 2: $f'(\eta)$ versus λ .

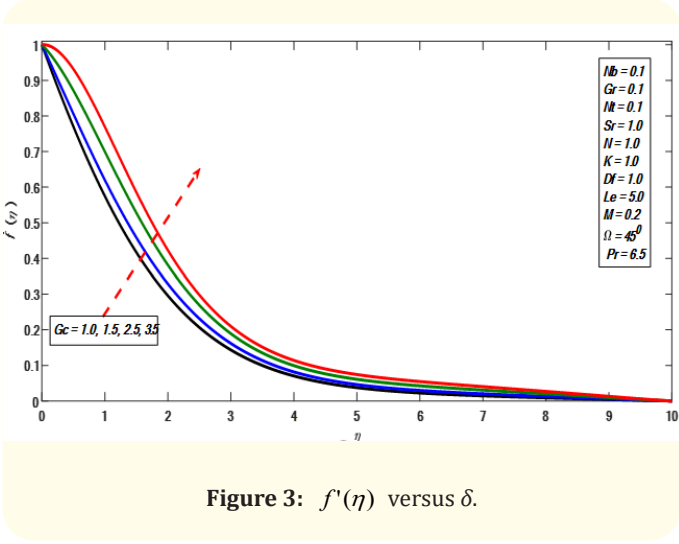
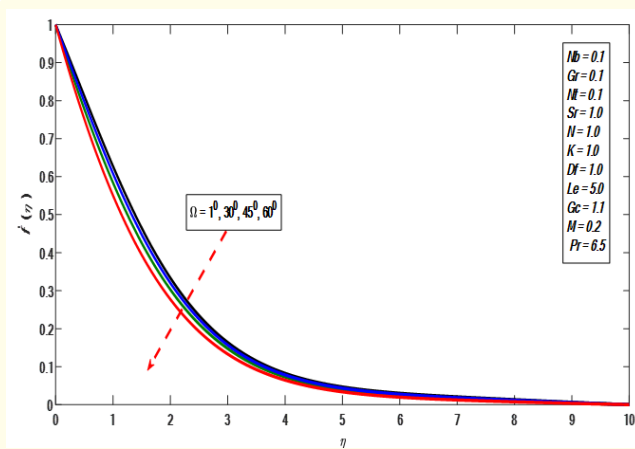
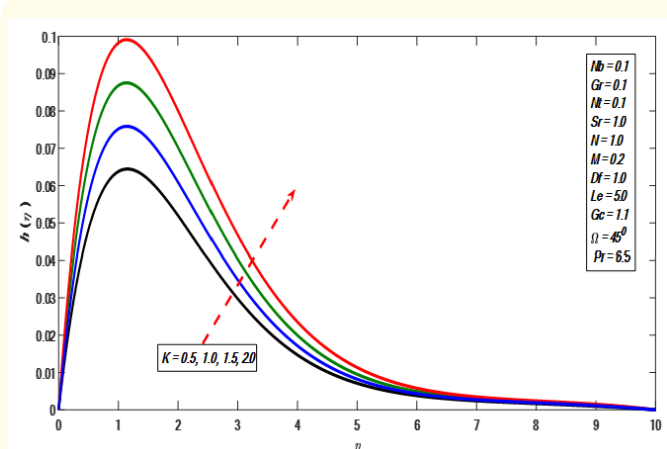
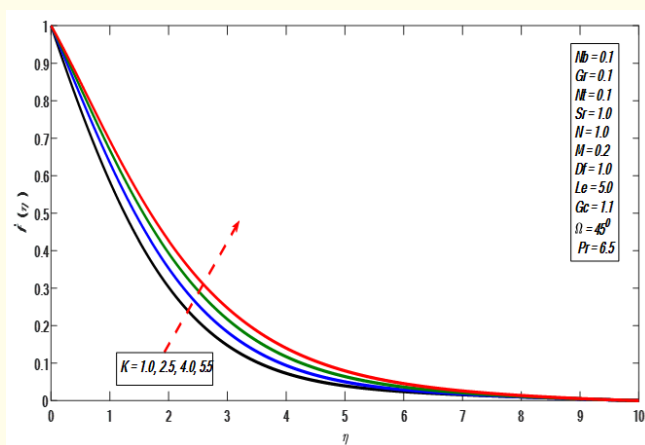
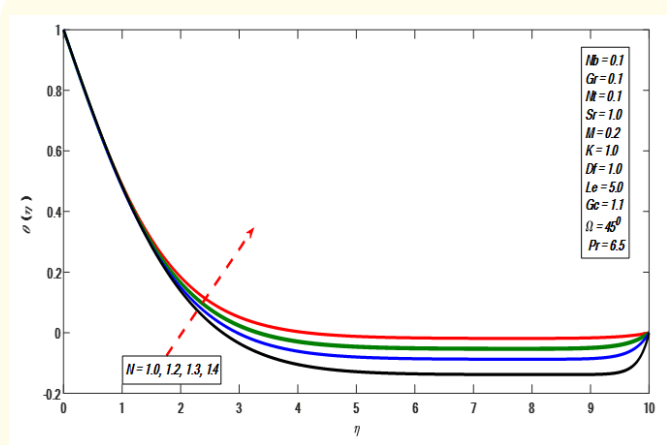
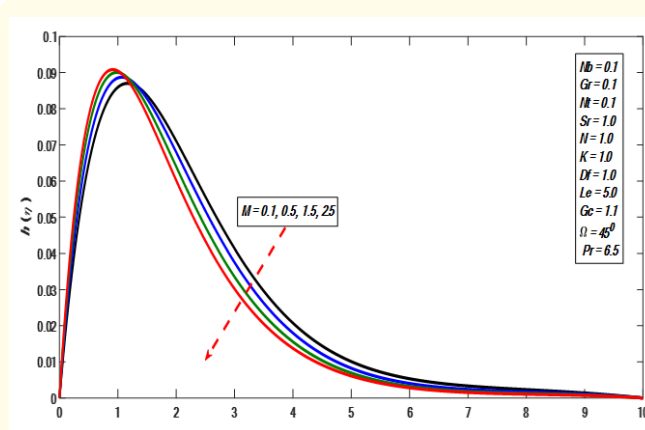
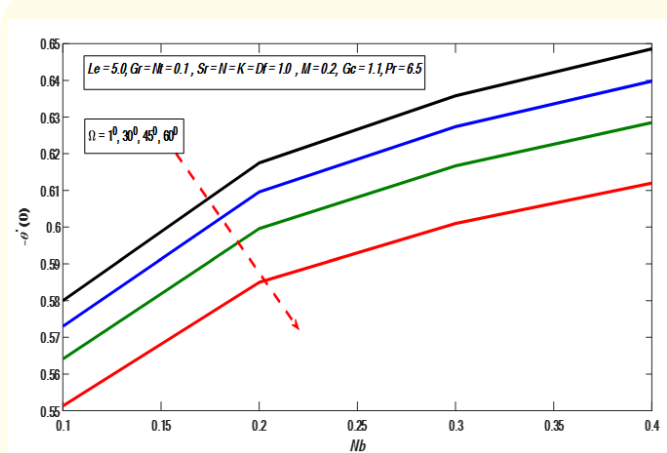
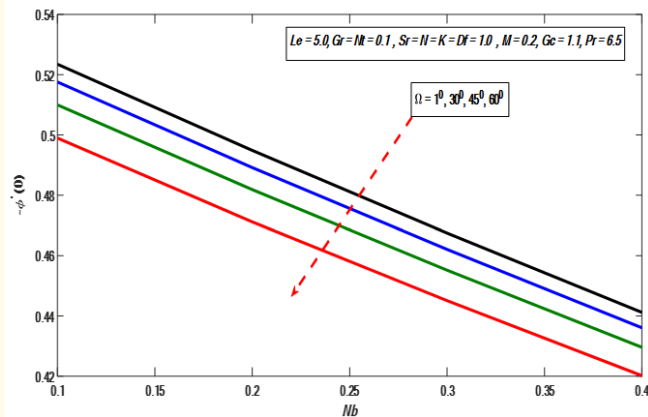
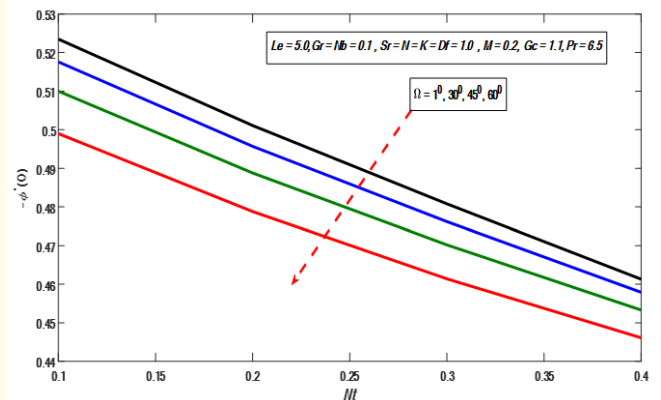
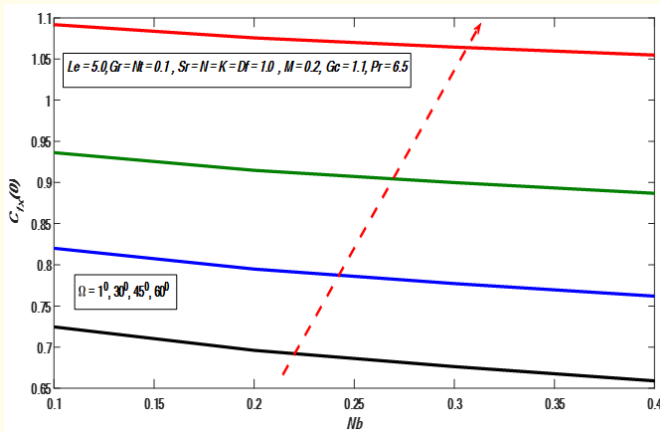
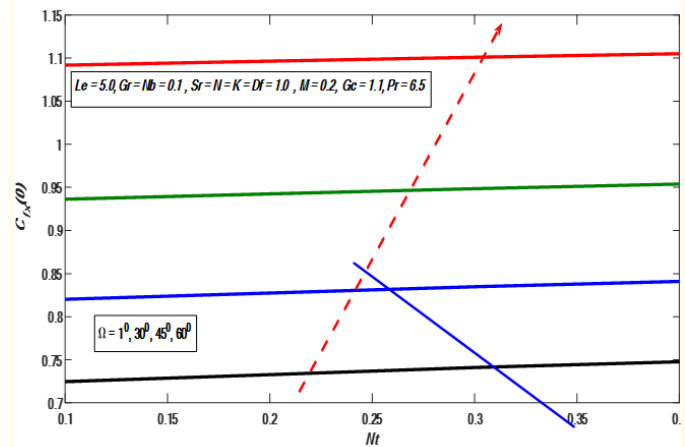
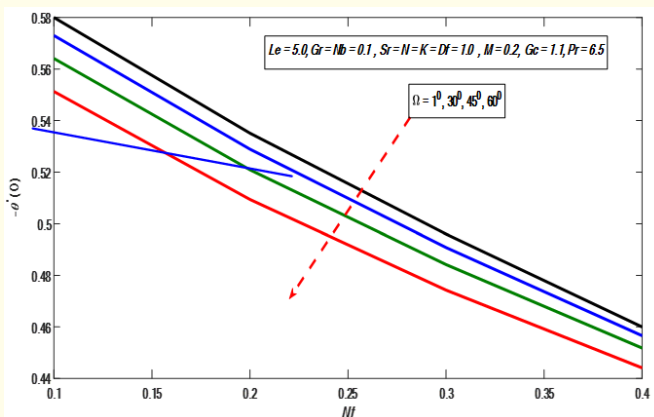


Figure 3: $f'(\eta)$ versus δ .


 Figure 4: $f'(\eta)$ versus Ω .

 Figure 7: $h(\eta)$ versus M .

 Figure 5: $f'(\eta)$ versus K .

 Figure 8: $\theta'(\eta)$ versus N .

 Figure 6: $h(\eta)$ versus M .

 Figure 9: $-\theta'(0)$ versus Nb and Ω .


 Figure 10: $-\theta'(0)$ versus Nb and Ω .

 Figure 13: $-\theta'(0)$ versus Nt and Ω .

 Figure 11: $-C_{fx}(0)$ versus Nb and Ω .

 Figure 14: $-C_{fx}(0)$ versus Nt and Ω .

 Figure 12: $-\theta'(0)$ versus Nt and Ω .

Conclusions

This research has been carried out for the micro-rotational effects on nano liquid flow over the slanted sheet which is extendable. The impacts of the radiations are visualized via graphs and numerically with the utilization of Keller box technique. This research is very useful for practical applications in the industry and engineering. Table 2 cleared the up and downs of energy and mass transport variations which is helpful for practical applications. The key findings in this work are listed below.

- Velocity field declines against inclination effect.
- The temperature field increases with the growth of the radiation effect.
- By increasing Brownian parameter and inclination effect the energy and mass flux diminishes.

- Skin friction rises by improving the inclination and Brownian effect.
- The buoyancy force impact increases the velocity field.
- Skin friction enhances by growing the thermophoretic.

Bibliography

1. Choi SU and Eastman J A. "Enhancing thermal conductivity of fluids with nanoparticles (No. ANL/MSD/CP-84938; CONF-951135-29)". Argonne National Lab., IL (United States) (1995).
2. Pak B C and Cho Y I. "Hydrodynamic and heat transfer study of dispersed fluids with submicron metallic oxide particles". *Experimental Heat Transfer an International Journal* 11.2 (1998): 151-170.
3. Buongiorno J. "Convective transport in nanofluids". *Journal of Heat Transfer* 128.3 (2006): 240-250.
4. Komeilibirjandi A., et al. "Thermal conductivity prediction of nanofluids containing CuO nanoparticles by using correlation and artificial neural network". *Journal of Thermal Analysis and Calorimetry* (2019): 1-11.
5. Toghyani S., et al. "Energy and exergy analyses of a nanofluid based solar cooling and hydrogen production combined system". *Renewable Energy* 141 (2019): 1013-1025.
6. Rashidi M M., et al. "Entropy generation in a circular tube heat exchanger using nanofluids: effects of different modeling approaches". *Heat Transfer Engineering* 38.9 (2017): 853-866.
7. Abdollahzadeh Jamalabadi M Y., et al. "Modeling of Subcooled Flow Boiling with Nanoparticles under the Influence of a Magnetic Field". *Symmetry* 11.10 (2019): 1275.
8. Abdollahzadeh Jamalabadi M Y., et al. "Effects of nanoparticle enhanced lubricant films in thermal design of plain journal bearings at high Reynolds numbers". *Symmetry* 11.11 (2019): 1353.
9. Rashidi M M., et al. "Entropy generation in a circular tube heat exchanger using nanofluids: effects of different modeling approaches". *Heat Transfer Engineering* 38.9 (2017): 853-866.
10. Sandeep N and Kumar M S. "Heat and Mass Transfer in Nanofluid Flow over an Inclined Stretching Sheet with Volume Fraction of Dust and Nanoparticles". *Journal of Applied Fluid Mechanics* 9.5 (2016).
11. Govindarajan A. "Radiative fluid flow of a nanofluid over an inclined plate with non-uniform surface temperature". In *Journal of Physics: Conference Series* 1000.1 (2018): 012173.
12. Khan I., et al. "Magnetohydrodynamics Carreau nanofluid flow over an inclined convective heated stretching cylinder with Joule heating". *Results in physics* 7 (2017): 4001-4012.
13. Saeed A., et al. "Three-Dimensional Casson Nanofluid Thin Film Flow over an Inclined Rotating Disk with the Impact of Heat Generation/Consumption and Thermal Radiation". *Coatings* 9.4 (2019): 248.
14. Maleki H., et al. "Heat transfer and nanofluid flow over a porous plate with radiation and slip boundary conditions". *Journal of Central South University* 26.5 (2019): 1099-1115.
15. Mabood F., et al. "Non-uniform heat source/sink and Soret effects on MHD non-Darcian convective flow past a stretching sheet in a micropolar fluid with radiation". *International Journal of Heat and Mass Transfer* 93 (2016): 674-682.
16. Maleki H., et al. "Heat transfer and nanofluid flow over a porous plate with radiation and slip boundary conditions". *Journal of Central South University* 26.5 (2019): 1099-1115.
17. Mjankwi M A., et al. "Unsteady MHD Flow of Nanofluid with Variable Properties over a Stretching Sheet in the Presence of Thermal Radiation and Chemical Reaction". *International Journal of Mathematics and Mathematical Sciences* (2019).
18. Muhammad S., et al. "Radiative Heat Transfer and Magneto Hydrodynamics Bioconvection Model for Unsteady Squeezing Flow of Nanofluid with Sort and Dufour Effects Between Parallel Channels Containing Nanoparticles and Gyrotactic Microorganisms". *Journal of Nanofluids* 8.7 (2019): 1433-1445.
19. Devi SA., et al. "Radiation effects on MHD boundary layer flow and heat transfer over a nonlinear stretching surface with variable wall temperature in the presence of non-uniform heat source/sink". *International Journal of Applied Mechanics and Engineering* 23.2 (2018): 289-305.
20. Eringen A C. "Simple microfluids". *International Journal of Engineering Science*, 2.2 (1964): 205-217.
21. Rafique K., et al. "Numerical Study on Micropolar Nanofluid Flow over an Inclined Surface by Means of Keller-Box". *Asian Journal of Probability and Statistics* (2019): 1-21.

22. Rafique K., *et al.* "Numerical Analysis with Keller-Box Scheme for Stagnation Point Effect on Flow of Micropolar Nanofluid over an Inclined Surface". *Symmetry* 11.11 (2019): 1379.
23. Kasim A R M., *et al.* "Unsteady MHD mixed convection flow of a micropolar fluid along an inclined stretching plate". *Heat Transfer—Asian Research* 42.2 (2013): 89-99.
24. Ghadikolaei S S., *et al.* "Nonlinear thermal radiation effect on magneto Casson nanofluid flow with Joule heating effect over an inclined porous stretching sheet". *Case Studies in Thermal Engineering* 12 (2018): 176-187.
25. Srinivasacharya D., *et al.* "Double dispersion effect on nonlinear convective flow over an inclined plate in a micropolar fluid saturated non-Darcy porous medium". *Engineering Science and Technology, an International Journal* 21.5 (2018): 984-995.
26. Soid S K., *et al.* "MHD stagnation-point flow over a stretching/shrinking sheet in a micropolar fluid with a slip boundary". *Sains Malaysiana* 47.11 (2018): 2907-2916.
27. Mishra S R., *et al.* "Free convective micropolar fluid flow and heat transfer over a shrinking sheet with heat source". *Case Studies in Thermal Engineering* 11 (2018): 113-119.
28. Gnaneswara Reddy M., *et al.* "Micropolar fluid flow over a nonlinear stretching convectively heated vertical surface in the presence of Cattaneo-Christov heat flux and viscous dissipation". *Frontiers in Heat and Mass Transfer (FHMT)* 8 (2017).
29. Abbas N., *et al.* "On stagnation point flow of a micro polar nanofluid past a circular cylinder with velocity and thermal slip". *Results in Physics* 9 (2018): 1224-1232.
30. Rafique K., *et al.* "Keller-Box Simulation for the Buongiorno Mathematical Model of Micropolar Nanofluid Flow over a Nonlinear Inclined Surface". *Processes* 7.12 (2019): 926.
31. Rafique K., *et al.* "Hydromagnetic Flow of Micropolar Nanofluid". *Symmetry* 12 (2020): 251.
32. Khan W A and Pop I. "Boundary-layer flow of a nanofluid past a stretching sheet". *International Journal of Heat and Mass Transfer* 53.11-12 (2010): 2477-2483.